

Random field based model of mixed ferroelectrics phase diagram

M.D.Glinchuk, E.A.Eliseev

Institute for Problems of Materials Science, NASc of Ukraine, Krjijanovskogo 3, 03180 Kiev, Ukraine

V.A.Stephanovich

*Institute of Semiconductor Physics NASc of Ukraine, Prospect Nauki 28, Kiev, Ukraine and
Institute of Mathematics University of Opole, Oleska 48, 45-052, Opole, Poland*

L.Jastrabik

*Institute of Physics, Academy of Sciences of the Czech Republic, Na Slovance 2, Prague, Czech Republic
(April 26, 2024)*

The equations for phase transitions temperatures, order parameters and critical concentrations of components have been derived for mixed ferroelectrics. The electric dipoles randomly distributed over the system were considered as a random field sources. We derive a random field distribution function for different orientations of the electric dipoles with nonlinear and spatial correlation effects included. The concentrational dependence of transition temperature for $A_{1-x}B_x$ mixed system has been calculated for A and B being antiferroelectric and ferroelectric materials as well as for A and B being ferroelectric and paraelectric. The numerical calculations have been carried out for $PbZr_{1-x}Ti_xO_3$ and $BaZr_xTi_{1-x}O_3$. The obtained results give a fairly good description of experimentally observed phase diagrams of these mixed systems. We discuss the physical reasons of strongly different behaviour of the systems related (in particular) to the relaxor properties appearance in $BaZr_xTi_{1-x}O_3$ at $x > 0.27$ and peculiar role of lead ions. We predict a transformation of any mixed system with ferroelectric (antiferroelectric) and paraelectric component into relaxor material at some large enough concentration of paraelectric component.

I. INTRODUCTION

There has been considerable amount of attention of scientists to mixed systems of different types like ferroelectric and antiferroelectric, ferroelectric and paraelectric etc due to their unusual physical properties, utilizable in many applications. A classic example of such a system is $PbZr_{1-x}Ti_xO_3$ (PZT) with broad range of its technical usage [1], including novel branches of electronics [9]. Most of the important peculiarities occur in the special regions of concentrations in the vicinity of different phase boundaries on phase diagram. In particular, for PZT the most interesting range is the morphotropic one with coexistence of ferroelectric phases with two different symmetries and antiferroelectric-ferroelectric phase boundary [9,10]. The characteristic features of phase diagram and properties anomalies depend essentially on the type of solid solution components (ferroelectric, antiferroelectric or paraelectric). It is especially interesting from this point of view to compare phase diagrams of PZT (solid solution of antiferroelectric $PbZrO_3$ and ferroelectric $PbTiO_3$) and $BaZr_xTi_{1-x}O_3$ (BZT, which is solid solution of ferroelectric $BaTiO_3$ and paraelectric $BaZrO_3$ [14]. The latter clearly demonstrates a peculiar role of lead ions in phase transitions of perovskite structure materials (see e.g. [16]). Due to different states (e.g. ferroelectric, paraelectric etc) of PZT and BZT components, their phase diagrams are strongly different (see e.g. [11,3]). Namely, several phases with long range order exist in PZT while BZT exhibits relaxor behaviour

beginning at $x = 0.27$. To find out the physical mechanisms "responsible" for actual phase diagram formation in mixed system, the theoretical calculations seem to be extremely desirable. Recently, the random field model for calculation of physical properties of mixed system had been proposed [17]. In the present work this model is expanded by taking into account the nonlinear and correlation effects as well as different orientations of the dipoles. This made it possible to calculate the concentration dependence of transition temperature, determine the symmetry of order parameters (and obtain the change of mixed system symmetry). This model also permits to obtain the range of parameters for existence of morphotropic region and appearance of glassy state. We apply this essentially improved model to calculations of phase diagrams of PZT and BZT. The theory describes adequately the observed phase diagram in these materials.

II. ORDER PARAMETERS

In the case of solid solutions of antiferroelectric and ferroelectric materials we have to consider three order parameters. Namely, in two-sublattice model for antiferroelectric component there are ferroelectric L_{2F} and antiferroelectric L_{2A} order parameters that describe, respectively, the homogeneous and inhomogeneous displacements of ions. The third order parameter L_{1F} is related to another component of solid solution. Keeping in mind the key role of electric dipoles in the system and their

ability to be oriented by electric field E we write the order parameters in the form inherent for Ising model [18]:

$$L_{1F}^{mf} = \tanh((d_1^*E + T_{1F}L_{1F})/T) \quad (1a)$$

$$L_{2F}^{mf} = \frac{1}{Z}[\sinh(2(d_2^*E + T_{2F}L_{2F})/T)] \quad (1b)$$

$$L_{2A}^{mf} = \frac{1}{Z}[\sinh(2T_{2A}L_{2A}/T)] \quad (1c)$$

$$Z = \cosh(2(d_2^*E + T_{2F}L_{2F})/T) + \cosh(2T_{2A}L_{2A}/T)$$

Here d_1^* and d_2^* are effective dipole moments related to the first ($x = 1$) and the second ($x = 0$) components; T_{1F} is ferroelectric phase transition temperature of the first component and T_{2F} , T_{2A} are the transition temperatures of ferroelectric and antiferroelectric phases of the second component of solid solution. Superscript "mf" in L shows that Eqs.(1) are written in a mean field approximation.

In the mixed system the positions of the dipoles of both components become random so that they can be considered as a random field sources. In this case order parameters given by Eqs. (1) have to be averaged with the random field distribution function $f(E, L_{1F}, L_{2F})$. Note, that in general case electric field E is the sum of external and internal field, but hereafter we suppose the absence of external field. Allowing for nonlinear and spatial correlation effects contribution into the distribution function, [5] order parameters for the mixed system can be written as:

$$L_{1F} = \int \tanh(d_1^*\varphi_1(\mathbf{E}\mathbf{e}_1)/T)f(\mathbf{E}, L_{1F}, L_{2F})d^3E, \quad (2a)$$

$$L_{2F} = \int \frac{\sinh(d_2^*\varphi_2(\mathbf{E}\mathbf{e}_2)/T)f(\mathbf{E}, L_{1F}, L_{2F})d^3E}{\cosh(d_2^*\varphi_2(\mathbf{E}\mathbf{e}_2)/T) + \cosh(2T_{2A}L_{2A}/T)}, \quad (2b)$$

$$L_{2A} = \int \frac{\sinh(2T_{2A}L_{2A}/T)f(\mathbf{E}, L_{1F}, L_{2F})d^3E}{\cosh(d_2^*\varphi_2(\mathbf{E}\mathbf{e}_2)/T) + \cosh(2T_{2A}L_{2A}/T)}, \quad (2c)$$

$$\varphi_i(E) = E(1 + \alpha_3^{(i)}E^2), \quad \mathbf{e}_i = \frac{\mathbf{d}_i^*}{|\mathbf{d}_i^*|}. \quad (2d)$$

Here $\varphi_i(E)$ is the nonlinear function of the field, which has the form of infinite series in odd powers of E in the lattices with a center of inversion in paraelectric phase. We keep in (2d) only first nonvanishing nonlinear term

$$f(\mathbf{E}) = \frac{1}{(2\pi)^3} \int \exp(i\rho(\mathbf{E} - \mathbf{E}_0) - x\Delta E_1^2(\mathbf{e}_1\rho)^2 - (1-x)\Delta E_2^2(\mathbf{e}_2\rho)^2) d^3\rho. \quad (4)$$

$$\mathbf{E}_0 = x\frac{T_{1F}}{d_1^*}L_{1F}\mathbf{e}_1 + (1-x)\frac{T_{2F}}{d_2^*}L_{2F}\mathbf{e}_2. \quad (5)$$

Here \mathbf{E}_0 is a mean field, ΔE_1 and ΔE_2 are the halfwidths of the distribution functions induced by d_1^* and d_2^* dipoles respectively. They can be written in the form [7]:

with the coefficient α_3 . Also, $f(E, L_{1F}, L_{2F})$ is a linear random field distribution function. It is seen, that in the case when both components are ferroelectrics, i.e. $L_{2A} = 0$, Eq.(2b) has the same form as Eq.(2a) as it has to be expected, but with different parameters. Therefore Eqs.(2) describe a quite general case. They give the order parameters dependence on the characteristics of mixed system components and their molar fractions via the random field distribution function. We would like to emphasize that the parameters L are the fraction ($0 \leq L \leq 1$) of coherently oriented dipoles of the mixed system components. Polarization \mathbf{P} as the actual order parameter of mixed system can be expressed via L_i as:

$$\mathbf{P} = \frac{x}{a_1^3}L_{1F}\mathbf{d}_1^* + \frac{1-x}{a_2^3}L_{2F}\mathbf{d}_2^*, \quad (3)$$

where a_1 , a_2 and x , $1-x$ are respectively lattice constants and molar fractions of the first and the second components in the solid solution with chemical formula $A_{1-x}B_x$. Note, that L_{2A} contributes neither to mixed system polarization nor to the random field distribution function as it has to be expected. The orientation of mixed system polarization is related to the vector sum of the dipoles in accordance with Eq.(3). To derive this sum coefficients, one has to calculate $L_{1,2F}$ on the base of Eqs.(2) which depend on the form of function $f(E, L_{1F}, L_{2F})$.

III. THE RANDOM FIELD DISTRIBUTION FUNCTION

As we have seen above, to calculate the nonlinear distribution function of random fields, it is sufficient to calculate the linear distribution function (i.e. that without nonlinear and spatial correlation effects). For latter purpose all kind of dipoles can be considered as independent sources of random field. Therefore, the distribution function of the mixed system is a convolution of the two types of dipoles distribution functions [6]. Gaussian approximation for these functions leads to the following expression for mixed system distribution function:

$$\Delta E_1^2 = \frac{16\pi}{15} \frac{d_1^{*2}}{\varepsilon_1^2 r_{c1}^3 a_1^3}, \quad \Delta E_2^2 = \frac{16\pi}{15} \frac{d_2^{*2}}{\varepsilon_2^2 r_{c2}^3 a_2^3}, \quad (6)$$

where ε_1 and r_{c1} , ε_2 and r_{c2} are dielectric permittivities and correlation radii of the solid solution components.

One can see from Eqs. (4), (5), (6) that mixed system distribution function depends on the components concen-

trations, order parameters L_{1F} L_{2F} , transition temperatures T_{1F} T_{2F} , their dipole moments and other physical parameters.

IV. PHASE DIAGRAM. GENERAL EQUATIONS.

The phase diagram has to reflect the variation of the transition temperatures of different phases with the in-

creasing of the fraction of the components as well as the phases symmetry changing. All this information can be obtained by solving the equations (2) with respect to Eqs. (4), (5). Substitution of Eq.(4) into (2) leads to six-fold integrals. They can be simplified due to the dependence of all the integrands on the scalar product $(\mathbf{E}\mathbf{e}_i)$, i.e. only on the parallel to \mathbf{e}_i field component. This permits to integrate out two other field components and to perform the integration over $d^3\rho$. This finally yields:

$$\begin{aligned} L_{1F} &= \int_{-\infty}^{+\infty} \tanh(d_1^* \varphi_1(E)/T) \exp\left(-\left(\frac{E-E_{01}}{2\Delta_1}\right)^2\right) \frac{dE}{2\sqrt{\pi}\Delta_1}, \\ L_{2F} &= \int_{-\infty}^{+\infty} \frac{\sinh(2d_2^* \varphi_2(E)/T)}{\cosh(2d_2^* \varphi_2(E)/T) + \cosh(2T_{2A}L_{2A}/T)} \exp\left(-\left(\frac{E-E_{02}}{2\Delta_2}\right)^2\right) \frac{dE}{2\sqrt{\pi}\Delta_2}, \\ L_{2A} &= \int_{-\infty}^{+\infty} \frac{\sinh(2T_{2A}L_{2A}/T)}{\cosh(2d_2^* \varphi_2(E)/T) + \cosh(2T_{2A}L_{2A}/T)} \exp\left(-\left(\frac{E-E_{02}}{2\Delta_2}\right)^2\right) \frac{dE}{2\sqrt{\pi}\Delta_2}, \end{aligned} \quad (7)$$

where $E_{0i} = (\mathbf{E}_0\mathbf{e}_i)$ ($i = 1, 2$), so that E_{0i} depends on the angle θ between the directions of the two types of dipoles, because $(\mathbf{e}_1\mathbf{e}_2) = \cos(\mathbf{e}_1, \mathbf{e}_2) \equiv \cos\theta$. The parameters Δ_i also depend on this angle, namely:

$$\begin{aligned} \Delta_1 &= x(\Delta E_1)^2 + (1-x)(\Delta E_2 \cos\theta)^2, \\ \Delta_2 &= x(\Delta E_1 \cos\theta)^2 + (1-x)(\Delta E_2)^2. \end{aligned} \quad (8)$$

The Eqs.(7) are the final form of the equations for the order parameters L_{2A} , L_{2F} , L_{1F} dependence on the molar fraction x and via them polarization of the system (see Eq.(3)). The transition temperature T_C to the ferroelectric phase and the transition temperature T_A to antiferroelectric one in the mixed system can be derived from Eq.(7) in the limit of zeroth order parameters. One can obtain from Eq.(7) the following system of equations:

$$L_{1F} = \frac{T_{1F}}{T_C} \left(xL_{1F} + (1-x) \frac{\cos\theta}{p\lambda} L_{2F} \right) I_1(T_C), \quad (9a)$$

$$L_{2F} = \frac{T_{2F}}{T_C} (p\lambda \cos(\theta)xL_{1F} + (1-x)L_{2F}) I_2(T_C), \quad (9b)$$

$$L_{2A} = \frac{T_{2A}}{T_A} (1-x)L_{2A} I_2(T_A), \quad (9c)$$

where

$$I_i(T) = \frac{1}{\sqrt{\pi}} \int_{-\infty}^{+\infty} \frac{(1+3\alpha_i(Q_i u)^2) \exp\left(-\frac{(u/2)^2}{T}\right)}{ch(Q_i u (1+\alpha_i(Q_i u)^2) T_{iF}/T)} du. \quad (10)$$

Here dimensionless variables are introduced:

$$\begin{aligned} p &= \frac{d_2^*}{d_1^*}, \quad \lambda_F = \frac{T_{1F}}{T_{2F}}, \quad \alpha_i = \alpha_3^{(i)} \left(\frac{T_{iF}}{d_i^*} \right)^2, \quad q_i = \frac{d_i^* \Delta E_i}{T_{iF}}, \quad \lambda_A = \frac{T_{2A}}{T_{2F}}, \\ Q_1^2 &= xq_1^2 + (1-x) \left(\frac{q_2 \cos\theta}{p\lambda_F} \right)^2, \quad Q_2^2 = x(q_1 p \lambda_F \cos\theta)^2 + (1-x)q_2^2. \end{aligned} \quad (11)$$

One can see that the temperature T_A follows from Eq.(9c), while the temperature T_C can be derived from Eqs.(9a), (9b). The solution of these equations has the form:

$$\begin{aligned} \tau_C &\equiv \frac{T_C}{T_{2F}} = \frac{1}{2} (x\lambda_F I_1(\tau_C) + (1-x)I_2(\tau_C) \pm \\ &\pm \sqrt{(x\lambda_F I_1(\tau_C))^2 + ((1-x)I_2(\tau_C))^2 + 2\cos(2\theta)\lambda_F x(1-x)I_1(\tau_C)I_2(\tau_C)}), \end{aligned} \quad (12a)$$

$$\tau_A \equiv \frac{T_A}{T_{2A}} = (1-x)I_2(\tau_A). \quad (12b)$$

The solution of Eqs (12) gives the dependences of T_C and T_A on molar fractions and material parameters of the mixed system components (see (11)).

V. COMPARISON OF THE THEORY AND EXPERIMENT

A. Phase diagram of $\text{PbZr}_{1-x}\text{Ti}_x\text{O}_3$

This solid solution components are antiferroelectric PbZrO_3 with transition temperature $T_{2A} = 503$ K (the value $T_{2F} \approx T_{2A}$ [18]) and ferroelectric PbTiO_3 with transition temperature from paraelectric phase to tetragonal ferroelectric phase $T_{1F} = 763$ K. Both components have electric dipoles randomly distributed in the mixed system. In accordance with the components symmetry one can suppose that $d_1^* \parallel [001]$ and $d_2^* \parallel [111]$ types of directions. Therefore parameters $\lambda_F \approx 1.516$, $\lambda_A = 1$ and $\cos \theta = 1/\sqrt{3}$. Other parameters were obtained from the fitting with observed phase diagram of PZT. We begin with the fitting of T_A from Eq.(12b). The numerical calculations of the integral I_2 were performed at $\alpha_2 = 0.3$, $q_2 = 2.9$. The dependence of T_A on molar fraction x is depicted by dashed line in Figure 1.

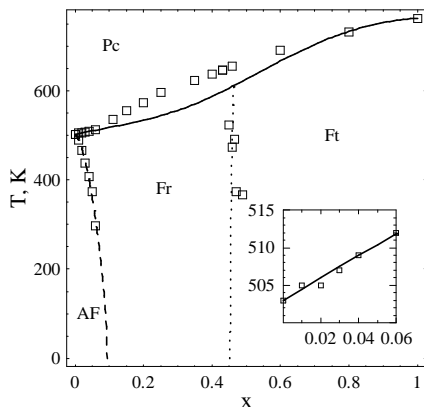


FIG. 1. Phase diagram of $\text{PbZr}_{1-x}\text{Ti}_x\text{O}_3$. Open squares are the experimental data [13]. Calculated transition temperatures are the following: solid line represents the transition from paraelectric phase (Pc) to ferroelectric phases (Fr, Ft), dashed line represents the transition from antiferroelectric phase (AF) to ferroelectric rhombohedral phase (Fr), dotted line represents the transition from (Fr) phase to ferroelectric tetragonal phase (Ft). The transition between Pc and Fr phases at small fractions x is depicted in inset.

One can see that T_A decreases with x increase and $T_A = 0$ K at $x = x_C = 0.093$ (where x_C is a critical frac-

tion at which antiferroelectric phase disappears). It is seen that the theory gives reasonable fit to experimental data shown by open squares in Figure 1. The transition temperature T_C calculated on the base of Eq.(12a) increases with x increase (see solid line in Figure 1). Our theory is undoubtedly valid at small x (see inset to Figure 1). The fitting of T_C for all the range of x were performed by varying of p , q_1 , q_2 , α_1 , α_2 . The best fit was achieved at $p = 0.828$, $q_1 = 0.239$, $q_2 = 0.364$, $\alpha_1 = 3.9$, $\alpha_2 = 4.3$. As it follows from Figure 1, the fitting is also good for $x > 0.6$, i.e. in the region enriched by titanium. For intermediate molar fractions $0.1 < x < 0.6$ the accuracy of the fitting is not so good as it is in the other regions.

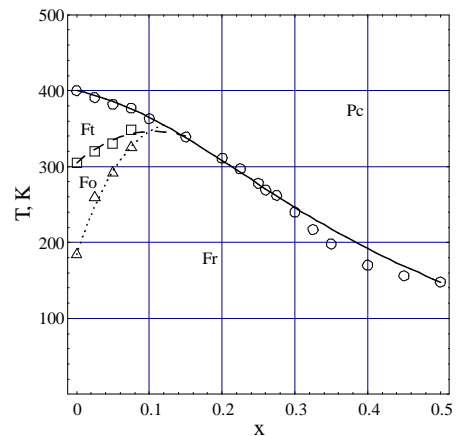


FIG. 2. Phase diagram $\text{BaZr}_x\text{Ti}_{1-x}\text{O}_3$. Open circles, squares and triangles are the experimental data from [3]. Calculated transition temperatures are the following: dashed line represents the transition between tetragonal (Ft) and orthorhombic (Fo) ferroelectric phases, dotted line represents the transition from (Fo) phase to ferroelectric rhombohedral phase (Fr), solid line represents the transition from paraelectric cubic phase (Pc) to (Ft, Fr) phases.

To our mind this deviation is related to the existence (in this interval of x) of additional order parameters originated from an improper ferroelectric phase transition. This transition occurs between high and low temperature rhombohedral phases. In the high temperature phase the spontaneous tilting of the oxygen octahedra causes the phase transition and contributes to the spontaneous polarization [11]. The symmetry of different ferroelectric phases and morphotropic region with both symmetries coexistence (see dotted line in Figure 1) was calculated on the base of Eqs. (3), (7), (8) with the same set of parameters as that used for the transition temperatures fitting. It is clear from Figure 1 that the morphotropic region lies between $x = 0.453$ at $T = 0$ K and $x = 0.463$ at $T = 611$ K. Therefore the calculations describe ade-

quately the observed phase diagram [13] represented by open squares in the Figure 1. Note that the best fit was obtained in the assumption that the halfwidths Δ_i of the distribution functions for each component are determined by the other component of solid solution. This confirms the supposition that the sources of the random field of the first component destroy the long-range order of the second component and vice versa.

B. Phase diagram of $\text{BaZr}_x\text{Ti}_{1-x}\text{O}_3$

The main component of this solid solution is the ferroelectric material BaTiO_3 which is known to have three phase transitions at $T_{2F}^{(1)} = 400$ K, $T_{2F}^{(2)} = 305$ K, $T_{2F}^{(3)} = 184$ K, to ferroelectric phases with tetragonal, orthorhombic and rhombohedral symmetries respectively. BaZrO_3 is paraelectric at all temperatures [14]. Phase diagram of BZT differs strongly from that of PZT. To describe it we proposed the following model.

We assume that in mixed BZT system zirconium ions can be shifted so that they supply the random electric dipoles to BaTiO_3 component. These dipoles are the main sources of the random field. This field distribution function halfwidth has to be larger than the mean field produced by zirconium dipoles because BaZrO_3 is paraelectric. Taking all these arguments into consideration we describe the phase diagram of BZT system with the help of Eqs.(3), (7), (8) with the following set of parameters:

$$\begin{aligned} T_{1F} &= 250 \text{ K}, & q_1 &= 0.6, & q_2 &= 0, & \alpha_1 &= 0; \\ \alpha_2^{(1)} &= 0.3, & p^{(1)} &= 2; & \alpha_2^{(2)} &= 2, & p^{(2)} &= 1.63; \\ \alpha_2^{(3)} &= 8, & p^{(3)} &= 1.25. \end{aligned} \quad (13)$$

Note, that it would be more accurate to write T_{1mf} instead of T_{1F} because there is no actual ferroelectric phase transition in BaZrO_3 .

Allowing for known symmetry of three BaTiO_3 ferroelectric phases, one can obtain $\cos(\theta^{(1)}) = 1$, $\cos(\theta^{(2)}) = 1/\sqrt{2}$, $\cos(\theta^{(3)}) = 1/\sqrt{3}$. The results of the calculation are shown in Figure 2. One can see that the theory describes the observed phase diagram (see [3] and references therein) quite well. Note, that the accuracy of fitting of experimental points by dashed and dotted lines at $x > 0.12$ is about 10%.

In Figure 3 we represented BZT order parameters calculated with the parameters (13) at $T = 0$ K. It is easy to check that in this limit $L_1 = L_2$. One can see that at $x > 0.3$ the fraction of coherently oriented dipoles L is less than 0.9 which corresponds to mixed ferroglass phase [4], the critical fraction for the dipole glass appearance ($L = 0$) being about $x_c \approx 0.82$. The relaxor behaviour (e.g. Vogel-Fulcher law in dynamic permittivity) was observed recently at $x \geq 0.27$ (see [3] and references therein).

The value of x_c for the transition to dipole glass state is a prediction of the theory. Unfortunately, the available experimental data cover the range up to $x = 0.5$. The clarification of dipole glass state existence may be performed in solid solution of BaTiO_3 and BaZrO_3 only under the condition of the components solubility in all the concentration range.

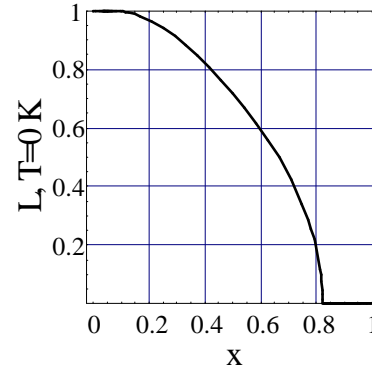


FIG. 3. The dependence of $\text{BaZr}_x\text{Ti}_{1-x}\text{O}_3$ order parameters at $T = 0$ K versus the molar fraction x .

VI. DISCUSSION

In the proposed model two components of the mixed system were considered as the materials with electric dipoles \mathbf{d}_1 and \mathbf{d}_2 . The dipoles tend to order the system along their directions so that the competition between different ordering directions is the main mechanism defining phase diagram of mixed system. Without this competition (when there is only one type of dipoles) it can be ferroelectric (PbTiO_3 , BaTiO_3), antiferroelectric (PbZrO_3) or paraelectric (BaZrO_3) phases. The difference between properties of the materials with Pb or Ba ions is related to peculiar role of lead ions in the phase transitions. In perovskite structure ABO_3 all A ions, but Pb, give almost no contribution to a lattice polarization. In contrast to this Pb ions contribution (e.g. in PbTiO_3) is the main one (see e.g. [16] and ref. therein). Opposite displacements of lead ions in PbZrO_3 are known to be the characteristic feature of antiferroelectric phase in PbZrO_3 . In our model \mathbf{d}_i represents the resultant dipole moment of a lattice unit cell. It is a vector sum of Pb and Ti ions displacements in the case of PbTiO_3 or Ti ions in BaTiO_3 , all the displacements being considered relatively oxygen cage. Therefore the extraction of lead contribution can be made only on the base of independent microscopic calculations or measurements of d_1^*/d_2^* ratio which is fitting parameter in our model. The estimation of this ratio with the help of known displacements (see e.g. [16]) of Ti ions in PbTiO_3 and Zr ions in PbZrO_3

gives $p = d_2^*/d_1^* \approx 0.8$ while our fit gives $p = 0.828$ (see section 5.1). Since nothing is known about Zr displacements in BaZrO_3 it is reasonable to calculate, e.g., the ratios of $k_1 = p_1/p_3$ and $k_2 = p_2/p_3$, which are independent on dipole moment of Zr ions. Under supposition that k_1 and k_2 can be estimated via the ratio of polarizations in ferroelectric phases of BaTiO_3 (see e.g. [12]), one obtains $k_1 = 1.8$, $k_2 = 1.4$ while in our model $k_1 = 1.6$, $k_2 = 1.3$ (see (13)). The values of p in (13) show that Zr displacement in BaZrO_3 is two times smaller, than that of Ti in tetragonal phase of BaTiO_3 . Therefore our model leads to reasonable values of the ions dipole moments both in PZT and BZT. It is actually possible to estimate fitting parameters with the help of Eqs.(6) provided that correlation radii and dipole moments are known. The parameters related to nonlinearity coefficients play an important role in description of peculiar form of BZT phase diagram because they are "responsible" for $T_c(x)$ maxima. Although the relation between $\alpha_2^{(i)}$ is qualitatively the same as that between nonlinearity constants α in different phases of BaTiO_3 (namely $\alpha_2^{(1)} < \alpha_2^{(2)} < \alpha_2^{(3)}$ (see (13)) and $\alpha^{(1)} < \alpha^{(2)} < \alpha^{(3)}$ [12]), quantitative estimation of $\alpha_2^{(i)}$ seems to be complex problem and the independent measurements of these parameters are desirable. Therefore these parameters are the actual fitting ones while other parameters could be estimated *a priori*. Another interesting feature of BZT phase diagram is appearance of relaxor behaviour at $x \geq 0.27$ while in PZT nothing of this kind is known. This may be related to the fact that in PbTiO_3 (due to lead ions displacements) spontaneous polarization is more than 2 times larger than that in BaTiO_3 [16]. As a result the random field induced by Zr ions appeared unable to destroy strong ferroelectric order in PbTiO_3 whereas in BaTiO_3 this field can destroy weaker ferroelectric long range order at large enough Zr ions concentration.

More generally we can assert that for a mixed system containing ferroelectric and paraelectric components, it has to be the concentration range where the system transforms into relaxor. This statement follows from the fact that paraelectric component contribution to mean field E_0 is rather small while it completely defines the distribution function half-width ($q_2 = 0$, see (13)). The contribution of the ferroelectric component to E_0 decreases (see Eq. (5) with subscripts 1 and 2 corresponding to paraelectric and ferroelectric component respectively and $T_{2A} = 0$, $L_{2A} = 0$ in Eqs. (7)). So, the increase of paraelectric component concentration leads to mean field decrease and to increase of distribution function half-width Δ (see Eqs. (6), (8)). This must result into $E_0/\Delta(x)$ decrease. In supposition that the state of a system (paraelectric (PE), ferroelectric (FE), dipole glass (DG), mixed ferroglass (FG) where FE long range order coexists with DG short range order) strongly depends on ratio E_0/Δ (see Figure 4), one can conclude that as x

increases, the system passes from FE to FG and than to DG state at some low temperature region (see arrows in Figure 4). Both FG and DG states are known to be characteristic feature of relaxor materials [4]. The relaxor systems exhibit nonergodic behaviour just in these phases. Vogel-Fulcher law which describes temperature dependence of dynamic dielectric susceptibility of relaxors can be related to the distribution of random electric fields in the mixed system [7]. The calculations of concentrational dependence of $(\text{BaTiO}_3)_{1-x}(\text{BaZrO}_3)_x$ order parameter made it possible to obtain the concentration ($x \approx 0.3$, see Figure 3) at which mixed system transforms into relaxor. It follows from Figure 3 that BZT is in FG phase at $0.3 < x < 0.8$ and could be in DG state at $x \geq 0.8$, the latter being dependent on existence of this x region in BZT mixed system. The existence of DG state and relaxor properties in another mixed system $(\text{BaTiO}_3)_{1-x}(\text{SrTiO}_3)_x$ (BST) at $x \geq 0.9$ [15] confirms the generality of the statement about transformation of mixed ferroelectric-paraelectric system into relaxor for some concentration range. This transformation seems to exist also in the mixed system consisting of antiferroelectric (component 2) and paraelectric (component 1). Really, from Eqs. (5), one can expect the decrease of E_0/Δ so the system at x increase passes from FE to FG and DG states (see the arrow in Figure 4). However, contrary to the case of ferroelectric-paraelectric mixed system, where T_{2F} is actual temperature of ferroelectric phase transition, in the above considered case T_{2F} is characteristic of "imaginary" ferroelectric phase following from two sublattice model of antiferroelectrics. Its value is close (although little lower) to T_{2A} [18].

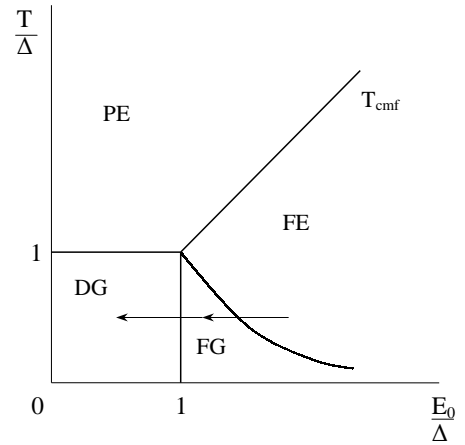


FIG. 4. Scheme of the disordered system phase diagram [2]

VII. CONCLUSION

We propose the random field based theory for calculation of phase diagram of mixed ferroelectrics and apply it to PZT and BZT materials. It has been shown that pro-

posed theoretical approach describes both qualitatively and quantitatively the observed phase diagrams, including relaxor behaviour in BZT at $x > 0.3$ (the measured fraction $x \approx 0.27$). This discrepancy may be related to the model assumption that electric dipoles of titanium and zirconium ions are the main sources of random fields. Zirconium ions can be considered as dilatation centers or elastic dipoles which are known to destroy a long-range order leading to relaxor properties appearance [4]. The calculations of latter property and of the contribution of oxygen octahedra tilting to the polarization of PZT are in progress now.

ACKNOWLEDGMENTS

Authors are grateful to Prof. T.Egami for fruitful discussions of the results.

-
- [1] Barfoot, J. C., and Tailor, G. W., 1979, *Polar Dielectric and Their Applications* (Macmillan Press).
- [2] Binder, K., and Young, A. P., 1986, *Rev. Mod. Phys.*, **58**, 801.
- [3] Farhi, R., El Marssi, M., Simon A., and Ravez, J., 1999, *Eur. Phys. J. B*, **9**, 599.
- [4] Glinchuk, M. D., and Farhi, R., 1996, *J. Phys.: Condens. Matter*, **8**, 6985.
- [5] Glinchuk, M. D., Farhi, R., and Stephanovich, V. A., 1997, *J. Phys.: Condens. Matter*, **9**, 10237.
- [6] Glinchuk, M. D., Grachev, V. G., Deigen, M. F., Roitsin, A. B., and Suslin, L. A., 1981, *Electricheskie Effecty v RadioSpectroscopii* (Moscow: Nauka).
- [7] Glinchuk, M. D., and Stephanovich, V. A., 1994, *J. Phys.: Condens. Matter*, **6**, 6317.
- [8] Glinchuk, M. D., and Stephanovich, V. A., 1999, *J. Appl. Phys.*, **85**, 1722.
- [9] Gundel, H. W., 1996, *Ferroelectrics*, **184**, 89.
- [10] Haertling, G. H., 1987, *Ferroelectrics*, **75**, 25.
- [11] Haun, M. J., Furman, E., Jang S. J., and Cross, L. E., 1989, *Ferroelectrics*, **99**, 13.
- [12] Iona, F., and Shirane, G., 1962, *Ferroelectric crystals* (Pergamon Press).
- [13] Jaffe, B., Cook, W. R., and Jaffe, H., 1971, *Piezoelectric Ceramics* (London and New York: Academic press).
- [14] Kenzig, W., 1957, *Ferroelectrics and Antiferroelectrics* (Publishers New York, Academic press Inc.).
- [15] Lemanov, V. V., Smirnova, E. P., Syrnikov, P. P., Tarakanov, E. A., 1996, *Phys. Rev. B*, **54**, 3151.
- [16] Lines, M. E., and Glass, A. M., 1977, *Principles and Application of Ferroelectric and Related Materials* (Oxford: Clarendon Press).
- [17] Stephanovich, V. A., Glinchuk, M. D., and Jastrabik, L., *Cond-mat /9907249*.
- [18] Vaks, V. G., 1973, *Vvedenie v microscopicheskuyu teoriyu segnetoelectricov* (Moscow: Nauka).